Available online at www.sciencedirect.com
SCIENCE DIRECT®
International Journal of Heat and Fluid Flow 25 (2004) 489–498
International Journal of HEAT AND FLUID FLOW
www.elsevier.com/locate/ijhff

Turbulence modification in gas–liquid and solid–liquid dispersed two-phase pipe flows

Shigeo Hosokawa *, Akio Tomiyama

Graduate School of Science and Technology, Kobe University, Rokkodai, Nada-ku, Kobe 657-8501, Japan

Abstract

The ratio ϕ of the eddy viscosity induced by the dispersed phase to the shear-induced eddy viscosity was confirmed to be an appropriate parameter for correlating turbulence modification in gas–solid two-phase pipe flows in our previous study. The purpose of this study is to examine the applicability of ϕ to gas–liquid and solid–liquid two-phase dispersed upflows in vertical pipes. Experiments were, therefore, conducted under various conditions, in which liquid, gas and solid volumetric fluxes, particle diameter and pipe diameter were chosen as parameters. The velocities of continuous and dispersed phases and the phase fractions were measured by LDV and an image processing method. It was confirmed that measured turbulence modification is better correlated with ϕ than with the critical parameter proposed by Gore and Crowe. The critical point at which no modification occurs is close to $\phi = 1$, irrespective of the type of two-phase dispersed flow.

Keywords: Turbulence modification; Dispersed two-phase flow; Eddy viscosity; Pipe flow; Bubble; Particle; LDV measurement

1. Introduction

Characteristics of a dispersed two-phase flow such as heat transfer and pressure drop cannot be well predicted without sufficient knowledge of two-phase turbulence. Many experimental studies have therefore been carried out to clarify characteristics of two-phase turbulence (Serizawa et al., 1975; Lance and Bataille, 1991), while paying attention to turbulence modification caused by the interaction between shear-induced turbulence and turbulence induced by the dispersed phase.

Serizawa and Kataoka (1988) carried out measurements of turbulence intensity in gas–liquid two-phase flows in vertical pipes and detected turbulence modification. Gore and Crowe (1989, 1991) investigated turbulence modification caused by the addition of particles in a gas flow, and pointed out that the modification is well correlated with the so-called critical parameter, d/l_t, the ratio of a particle diameter d to a turbulence length scale l_t. They applied this parameter to turbulence modification caused by bubbles and drops and confirmed that d/l_t is also applicable to gas–liquid dispersed flows. They also reported that the critical parameter refers only to the question of increase or decrease in turbulence intensity and does not relate to the magnitude of the change. The critical parameter can be regarded as the ratio of a characteristic length scale of turbulence induced by the dispersed phase to that of shear-induced turbulence. However the modification may depend not only on the length scales but also on the eddy viscosities of shear-induced turbulence and turbulence induced by the dispersed phase. Since the eddy viscosity might be one of the most fundamental quantities representing turbulence characteristics, the ratio ϕ of the eddy viscosity ν_d induced by the dispersed phase to the shear-induced eddy viscosity ν_t would be a candidate for the index of turbulence modification. To examine whether or not ϕ is an appropriate parameter for correlating turbulence modification, Hosokawa et al. (1998) measured turbulence intensities for gas–solid two-phase flows in a vertical pipe using several particles with different relative velocities, and confirmed that measured turbulence modification was well correlated with ϕ.

The applicability of ϕ to gas–liquid and solid–liquid two-phase dispersed upflows in vertical pipes was

* Corresponding author. Tel./fax: +81-78-803-6132.
E-mail addresses: hosokawa@mech.kobe-u.ac.jp (S. Hosokawa), tomiyama@mech.kobe-u.ac.jp (A. Tomiyama).

0142-727X/$ - see front matter © 2004 Elsevier Inc. All rights reserved.
doi:10.1016/j.ijheatfluidflow.2004.02.001

Nomenclature

D	pipe diameter (m)
C_{TI}	dimensionless change in turbulence intensity (–)
J	volumetric flux (m/s)
N_{d}	number density of dispersed phase (1/m^3)
P	pressure (Pa)
R	pipe radius (m)
Re	Reynolds number (–)
Re_{d}	particle/bubble Reynolds number (–)
Re_{t}	turbulence Reynolds number (–)
T	sampling time (s)
V_{T}	terminal velocity in stagnant water (m/s)
d	mean diameter of dispersed phase (m)
$g(\tau)$	autocorrelation function (–)
l_{t}	turbulence length scale (m)
r	radial position (m)
t	time (s)
u	local instantaneous velocity (m/s)
$\bar{u}$	mean velocity (m/s)
u'	turbulent fluctuation velocity (m/s)
u'', v'', w''	fluctuating velocity (m/s)
u_{r}	relative velocity between two phases (m/s)
x	spatial coordinate (m)
Φ	eddy viscosity ratio (–)
α_{d}	phase fraction of dispersed phase (–)
ν	kinematic viscosity (m^2/s)
ν_{d}	eddy viscosity induced by dispersed phase (m^2/s)
ν_{t}	shear-induced eddy viscosity (m^2/s)
ν_{tpf}	eddy viscosity in two-phase flow (m^2/s)
ρ	fluid density (kg/m^3)
ϕ	estimated value of eddy viscosity ratio (–)
φ	tangential coordinate (m)

Subscripts

G	gas phase
L	liquid phase
S	solid phase
d	dispersed phase
i, j	direction in Cartesian coordinates
t	shear-induced turbulence in single-phase flow
water	water

examined in this study. LDV measurements were carried out to obtain local instantaneous velocities and turbulence intensities of the continuous phase. To examine the effects of ϕ on turbulence modification, particles of three size classes were used for solid–liquid two-phase flows and experiments for gas–liquid two-phase flows were carried out by taking the liquid volumetric flux as a parameter.

2. Eddy viscosity ratio

The eddy viscosity ratio can be deduced from the following averaged Navier–Stokes equation for incompressible two-phase flow, which is based on ensemble average and the so-called eddy viscosity assumption (Delhaye et al., 1981):

$$\frac{\partial \bar{u}_i}{\partial t} + \bar{u}_j \frac{\partial \bar{u}_i}{\partial x_j} = -\frac{1}{\rho}\frac{\partial \overline{P}}{\partial x_i} + \frac{1}{\alpha}\frac{\partial}{\partial x_j}\alpha(\nu + \nu_{\mathrm{tpf}}) \times \left(\frac{\partial \bar{u}_i}{\partial x_j} + \frac{\partial \bar{u}_j}{\partial x_i}\right) - \frac{M_i}{\alpha\rho} \tag{1}$$

where the subscript i or j denotes the direction in Cartesian coordinates, u the fluid velocity, t the time, x the spatial coordinate, ρ the fluid density, P the pressure, α the phase fraction, ν the kinematic viscosity, ν_{tpf} the eddy viscosity of the two-phase flow. The bar represents the averaged quantity. The ν_{tpf} can be related with the eddy viscosity ν_{t} of shear-induced turbulence, the eddy viscosity ν_{d} induced by the dispersed phase, and the viscosity ν of the continuous phase. Hence, it can be expressed as

$$\nu_{\mathrm{tpf}} = f(\nu_{\mathrm{t}}, \nu_{\mathrm{d}}, \nu, \ldots) \tag{2}$$

Since the magnitude of ν is much smaller than those of ν_{t} and ν_{d}, one of the most significant dimensionless groups deduced from Eq. (2) would be

$$\Phi = \frac{\nu_{\mathrm{d}}}{\nu_{\mathrm{t}}} \tag{3}$$

The magnitude of ν_{d} can be evaluated as the product of the relative velocity between the phases and the mean diameter d of dispersed bubbles, drops or particles (Sato and Sekoguchi, 1975):

$$\nu_{\mathrm{d}} \propto u_{\mathrm{r}} d \tag{4}$$

where u_{r} is the absolute value of the difference between the local mean velocity of the continuous phase $\bar{u}$ and that of the dispersed phase $\bar{u}_{\mathrm{d}}$:

$$u_{\mathrm{r}} = |\bar{u} - \bar{u}_{\mathrm{d}}| \tag{5}$$

When the phase fraction of the dispersed phase α is low, the shear-induced eddy viscosity in a two-phase flow can be evaluated as the eddy viscosity in a single-phase flow with the same volumetric flux of the continuous phase as the two-phase flow. Hence, the magnitude of ν_{t} can be estimated as the product of the turbulence length scale l_{t} and the turbulent fluctuation velocity u'_{t} for the single-phase flow as follows:

$$\nu_t \propto u'_t l_t \tag{6}$$

where u'_t is the root mean square (RMS) value of the local instantaneous velocity u_t:

$$u'_t = \sqrt{\overline{(u_t - \bar{u}_t)^2}} \tag{7}$$

Hence, the magnitude of the eddy viscosity ratio Φ can be estimated as

$$\Phi \sim \phi \equiv \frac{u_r d}{u'_t l_t} \tag{8}$$

The estimated value ϕ of the eddy viscosity ratio can be understood as the product of Gore and Crowe's parameter and the ratio of the turbulence intensity caused by the dispersed phase to that by shear-induced turbulence. Let us refer to ϕ as the eddy viscosity ratio hereafter. Serizawa and Kataoka (1995) reported that turbulence modification in gas–liquid two-phase bubbly flows depends on the liquid volumetric flux J_L, in other words, on the intensity of shear-induced turbulence. Hosokawa et al. (1998) reported that turbulence modification in gas–solid two-phase flows depends on u_r. Due to the lack of u'_t and u_r, d/l_t cannot explain these results, whereas ϕ possesses a potential of correlating the effects of u'_t and u_r on turbulence modification. It should be also noted that ϕ is regarded as the ratio of the particle/bubble Reynolds number $Re_d \times (= u_r d/\nu)$ to the turbulence Reynolds number $Re_t (= u'_t l_t/\nu)$.

In Section 4, the eddy viscosity ratio will be correlated with a dimensionless change in turbulence intensity, C_{TI}, which is defined by (Gore and Crowe, 1989)

$$C_{TI} = \frac{\frac{u'}{\bar{u}} - \frac{u'_t}{\bar{u}_t}}{\frac{u'_t}{\bar{u}_t}} \tag{9}$$

where u' denotes the turbulent fluctuation velocity of the continuous phase in a two-phase flow, $\bar{u}$ the mean velocity of the continuous phase in a two-phase flow and $\bar{u}_t$ the mean velocity in a single-phase flow with the same liquid volumetric flux as the two-phase flow. The C_{TI} would increase with the number density, N_d, of dispersed phase even if ϕ is constant. Hence, C_{TI} per unit number density, C_{TI}/N_d, might be more appropriate than C_{TI} as the index of change in turbulence intensity. The number density N_d and the turbulence change per unit number density are defined by

$$N_d = \frac{6\alpha_d}{\pi d^3} \tag{10}$$

$$\frac{C_{TI}}{N_d} = \frac{\pi d^3}{6\alpha_d}\left(\frac{\frac{u'}{\bar{u}} - \frac{u'_t}{\bar{u}_t}}{\frac{u'_t}{\bar{u}_t}}\right) \tag{11}$$

where α_d is the phase fraction of dispersed phase.

3. Experimental apparatus and conditions

The experimental apparatus is shown in Fig. 1. Water, air and ceramic particles were used as continuous, gas and solid phases, respectively. Water was supplied from the Mohno pump, and flowed in the upward direction in the vertical pipe made of acrylic resin. The length and inner diameter of the pipe were 10 m and 30 mm, respectively. In the case of gas–liquid two-phase flows, air was supplied from the compressor and mixed with water at the mixing section located at the inlet of the vertical pipe. For liquid–solid two-phase flows, spherical solid particles were added to the flow using the feeder. Measurements were carried out at the location 7.5 m above the bottom of the pipe. The experimental conditions are summarized in Table 1. To examine the effects of shear-induced turbulence and diameter of dispersed phase on turbulence modification, experiments of gas–liquid two-phase flows were carried out under three conditions with different liquid volumetric fluxes. Particles of three size classes were used for the solid–liquid two-phase flow experiments. Experiments of bubbly flows in a vertical pipe, the diameter and length of which were 20 mm and 2 m, were also carried out to examine the effect of pipe diameter D on turbulence modification.

LDV measurements (DANTEC 60X83) were carried out to obtain axial velocities of liquid and solid phases. The uncertainty estimated at 95% confidence of measured velocity was 1% (DANTEC, 1993). Phase discrimination is indispensable to obtain accurate data. In the gas–solid two-phase flow experiments, two laser

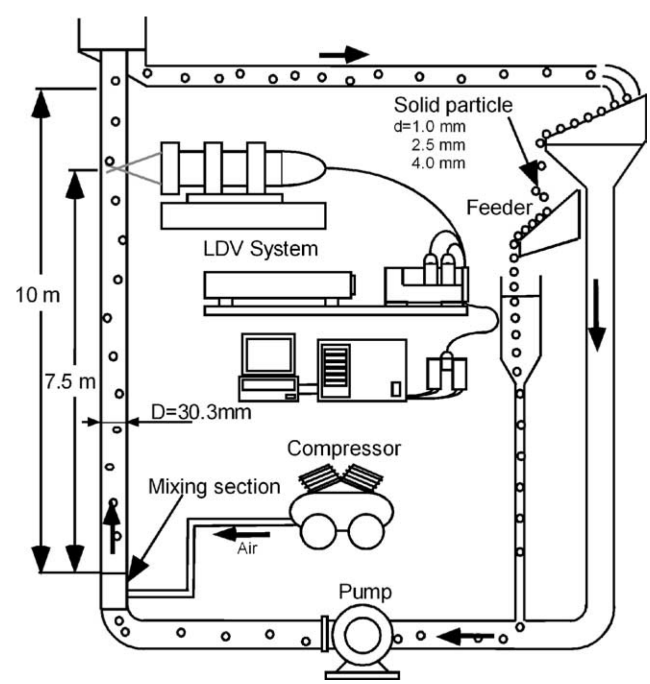

Fig. 1. Experimental apparatus.

Table 1
Experimental conditions

D (mm)	J_L (m/s)	Re	J_G (m/s)	d (mm)	σ_d (mm)	V_T (m/s)	$\langle\alpha_d\rangle$
Gas–liquid (air–water)							
30	0.5	1.5×10^4	0.017	4.9	0.67	0.28	2.2×10^{-2}
			0.023	4.9	0.64	0.28	3.0×10^{2}
30	0.7	2.1×10^4	0.017	4.8	0.66	0.28	1.9×10^{-2}
			0.023	4.8	0.68	0.28	2.7×10^{-2}
30	1.0	3.0×10^4	0.017	4.7	0.65	0.27	1.5×10^{-2}
			0.023	4.7	0.67	0.27	2.2×10^{-2}
20	0.5	1.0×10^4	0.015	3.7	0.62	0.24	1.9×10^{-2}
	0.9	1.8×10^4	0.020	3.2	0.70	0.25	1.9×10^{-2}
			J_S (m/s)				
Solid–liquid (water–ceramic particle 3200 kg/m^3)							
30	0.50	1.5×10^4	0.004	4.0	0.18	0.42	1.8×10^{-2}
				2.5	0.10	0.30	1.7×10^{-2}
				1.0	0.04	0.21	1.0×10^{-2}
			0.002	4.0	0.18	0.42	0.8×10^{-2}
				2.5	0.10	0.30	0.8×10^{-2}
				1.0	0.04	0.21	0.7×10^{-2}

J_L: liquid volumetric flux, $Re = J_L D/\nu$, J_G: gas volumetric flux, J_S: solid volumetric flux, V_T: terminal velocity, σ_d: standard deviation of d, $\langle\alpha_d\rangle$: area-averaged volume fraction of dispersed phase.

beams emitted from the LDV probe passed through the test section and were received by two photo-multipliers (DANTEC 55X08) as shown in Fig. 2 to detect the presence of a particle in the LDV measurement volume. The signals of photo-multipliers were recorded by a digital recorder (TEAC DRF1) which was synchronized with an LDV signal processor (DANTEC 58N10). When a particle exists at the measurement volume, the signals detected by the photo-multipliers indicate a low intensity due to the cutoff of laser beams as shown in Fig. 3. Measured liquid velocities u_L during the simultaneous decrease of the signals, which are denoted by triangle symbols in the figure, were rejected from the velocity data used for the calculation of mean velocity and turbulence intensity.

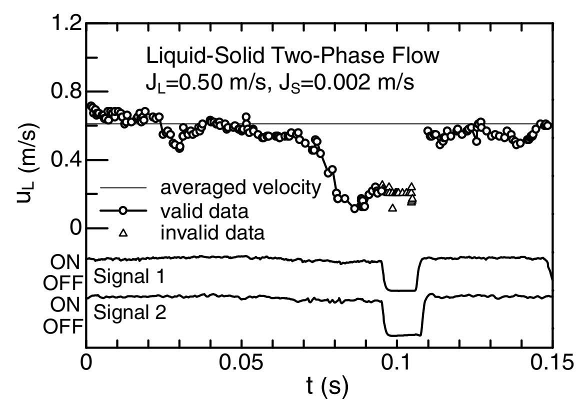

Fig. 3. An example of velocity data together with on–off signals.

In the gas–liquid two-phase flow experiments, the phase density function and liquid velocity were simultaneously measured by using a fluorescence technique, which enabled us the phase discrimination. A schematic of the measurement system is shown in Fig. 4. To measure the phase density function, Rhodamine B (a fluorescent dye) was dissolved in water. The phase density function was measured by using the intensity of fluorescence induced by the laser beams. When the measurement volume of LDV was filled with water, the LDV probe detected strong fluorescence, the wavelength λ of which was 590 nm, in addition to two Doppler signals ($\lambda = 488$ and 514.5 nm) from tracer particles. The three signals were splitted by a color separator and detected by three photo-multipliers. When the gas phase filled the measurement volume, no fluorescence was emitted from the measurement volume. The time series data of fluorescence intensity were digitized and stored in a digital recorder (Yokogawa AR1200), which provided the phase density function. Fig. 5 shows an example of the fluorescence signal and bubble images recorded by a high speed camera. The fluorescence signal quickly decreases when the bubble touches the measurement volume and quickly increases when the bubble passes through the measurement volume. Local instantaneous velocities were calculated by the LDV signal processor, which was

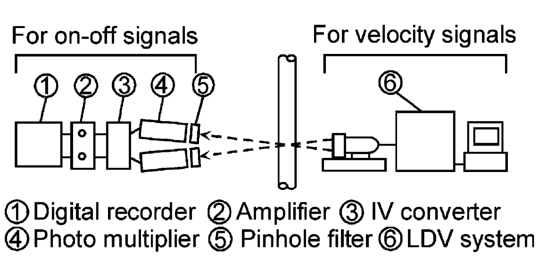

Fig. 2. Schematic of measurement system for gas–solid flows.

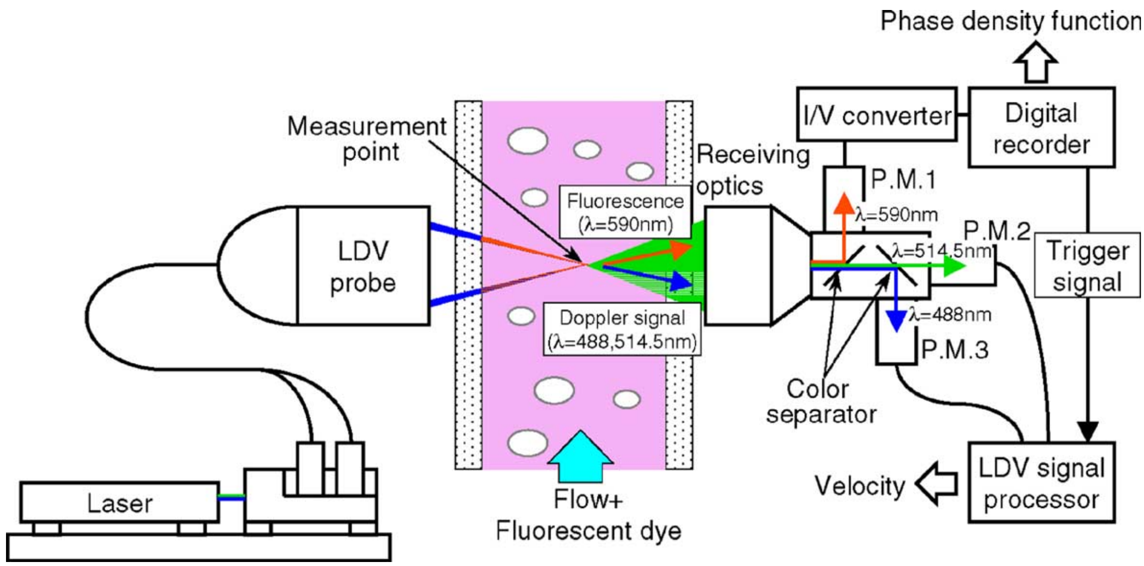

Fig. 4. Schematic of measurement system for gas–liquid flows.

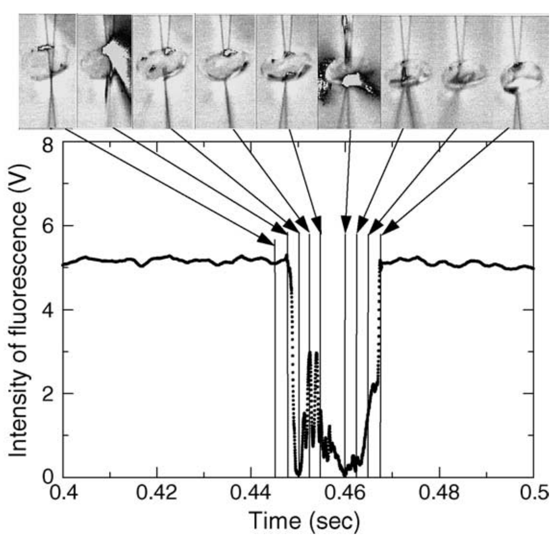

Fig. 5. An example of fluorescence signal together with bubble images.

synchronized with the digital recorder. The velocity data, which were obtained when the fluorescence signal was low due to the presence of a bubble in the measurement volume, were excluded from the liquid velocity data. It should be noted that bubble shapes under the present experimental condition were not spherical as shown in Fig. 5, which might be one of the main differences between the gas–liquid and the liquid–solid flows. The effects of this difference on the turbulence modification will be discussed in Section 4.2.

An image processing method was used to measure the bubble velocity, local and area-averaged gas-phase fractions, α_G and $\langle\alpha_G\rangle$, and mean diameter of bubbles. The uncertainties of bubble velocity and diameter estimated at 95% confidence were less than 2.5%, which was evaluated from the spatial resolution (0.063 mm/pixel) of the bubble image taken by a CCD camera (Kodak Motion Corder SR-1000). The uncertainties of α_G and $\langle\alpha_G\rangle$ were estimated by comparing gas-phase fractions measured by the image processing method and a conductance probe (KANOMAX, Model 0582, System 7931), and were evaluated as 5%. The area-averaged solid-phase fractions $\langle\alpha_S\rangle$ in solid–liquid flows were evaluated as the ratio of the solid volumetric flux J_S to the solid-phase averaged velocity $\overline{\overline{u_S}}$ which was calculated from the measured local mean velocity of the solid phase. Radial distributions of local solid-phase fraction, α_S, were evaluated using the local liquid velocity and the data rate of solid velocity, i.e., the number of particles passing through the measurement volume per unit time. The solid-phase fraction α_S thus obtained agreed well with α_S measured by the image processing method. The eddy viscosity ratio defined by Eq. (8) includes the turbulence length scale l_t in a single-phase flow. Since l_t is an unknown parameter, most of the previous studies adopted a model or empirical correlation to evaluate l_t. In the present study, high data rate measurements enabled us to evaluate l_t by substituting the measured $u_t(t)$ for single-phase flow conditions into the following equation:

$$l_t = \int_0^\infty g(\tau)\,d\tau \tag{12}$$

$$g(\tau) = \frac{1}{u_t'^2}\lim_{T\to\infty}\frac{1}{T}\int_0^T [u_t(t) - \bar{u}_t][u_t(t+\tau) - \bar{u}_t]\,dt \tag{13}$$

where $g(\tau)$ is the autocorrelation function of the fluctuating velocity and T the sampling time. The turbulence length scale l_t evaluated with Eqs. (12) and (13) is shown in Fig. 6 together with the length scale evaluated by

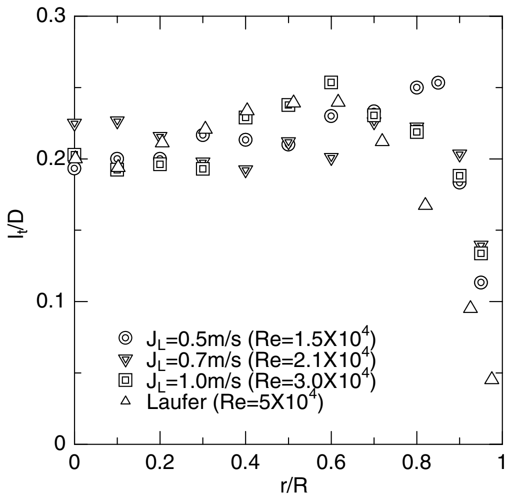

Fig. 6. Measured turbulence length scale l_t in single-phase flows ($D = 30$ mm).

substituting Laufer's data (1954) into the following expression of l_t proposed by Townsend (1956):

$$l_t = \frac{(2k)^{3/2}}{3\varepsilon} \tag{14}$$

where k is the turbulence kinetic energy and ε the rate of turbulence energy dissipation. The latter was evaluated by using the following equation (Hinze, 1959, Laufer, 1954):

$$\varepsilon = \nu\left\{\overline{\left(\frac{\partial u''}{\partial x}\right)^2} + \overline{\left(\frac{\partial v''}{\partial x}\right)^2} + \overline{\left(\frac{\partial w''}{\partial x}\right)^2} + 2.5\overline{\left(\frac{\partial u''}{\partial r}\right)^2} + 2.5\frac{1}{r^2}\overline{\left(\frac{\partial u''}{\partial \varphi}\right)^2}\right\} \tag{15}$$

where, u'', v'' and w'' denotes the components of fluctuating velocity in the axial, radial and tangential directions, respectively. The x, r and φ are the axial, radial and tangential coordinates, respectively. As shown in Fig. 6, the measured l_t agreed well with l_t based on Laufer's data, and therefore the measured length scale was used to evaluate the eddy viscosity ratio ϕ.

4. Results and discussion

4.1. Mean velocity and turbulence intensity

Measured axial liquid velocities $\bar{u}$ and RMS values u' normalized by the liquid volumetric flux J_L for gas–liquid two-phase flows in a 30-mm-dia. pipe are shown in Fig. 7. The liquid is accelerated due to the presence of bubbles, especially in the near wall region. The turbulence is also enhanced due to the presence of bubbles, and the augmentation is larger in the core region than in the near wall region, in spite of wall-peaking profile of

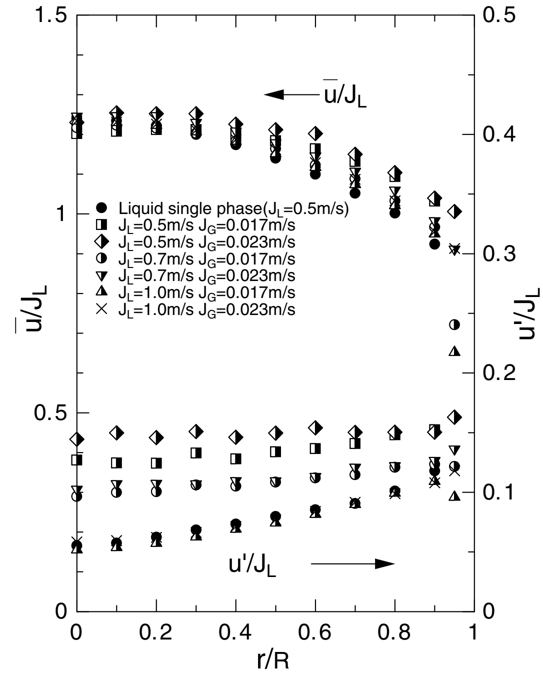

Fig. 7. Mean velocity and RMS in gas–liquid flow.

α_G. As a result, the distributions of u' become flattened in gas–liquid two-phase flows.

As shown in Fig. 8, C_{TI} and C_{TI}/N_d are much larger in the core region than in the near wall region. They increase with decreasing J_L, i.e., decreasing intensity of shear-induced turbulence. On the contrary, C_{TI}/N_d depends little on the gas volumetric flux J_G. Since bubble sizes and relative velocities between the phases are almost constant in the present experimental conditions,

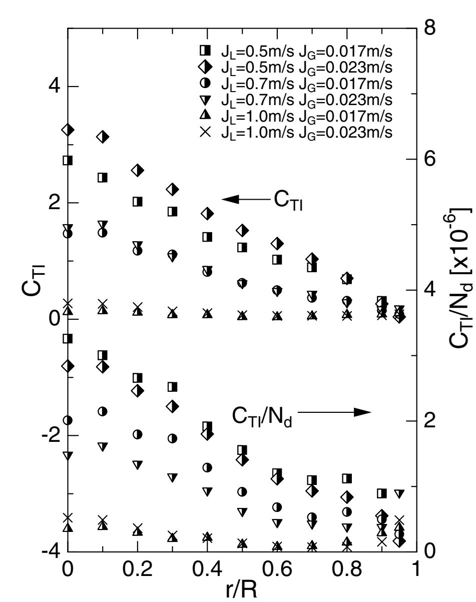

Fig. 8. Turbulence modification in gas–liquid flow.

the eddy viscosity ratio increases with decreasing shear-induced turbulence. This implies that C_{TI}/N_d increases with ϕ.

In the case of liquid–solid two-phase flows, the liquid velocity is accelerated, especially in the core region, as shown in Fig. 9. The turbulence also enhances due to the presence of particles and C_{TI} is more or less uniform over the cross section as shown in Fig. 10. On the other hand, C_{TI}/N_d is strongly augmented in the core region. It depends on d but little depends on J_S. The increase with d implies that C_{TI}/N_d increases with the length scale of particle-induced turbulence. Since J_L is kept constant in the experiments of liquid–solid flows, ϕ increases with d. The increase in ϕ therefore corresponds to the increase in C_{TI}/N_d.

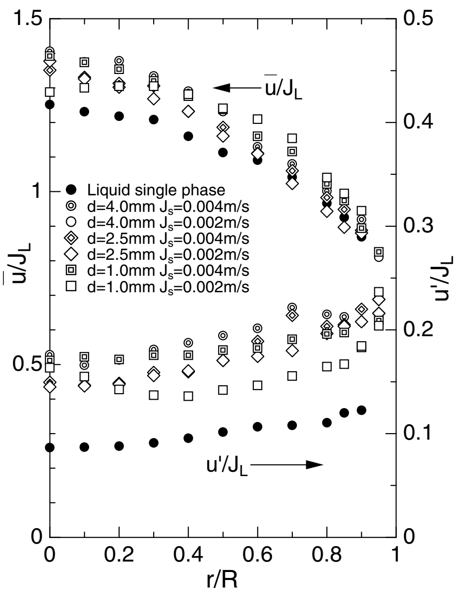

Fig. 9. Mean velocity and RMS in liquid–solid flow ($J_L = 0.5$ m/s).

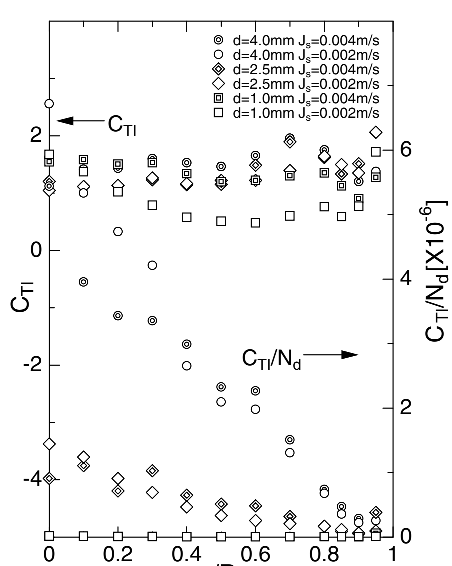

Fig. 10. Turbulence modification in liquid–solid flow ($J_L = 0.5$ m/s).

4.2. Correlation between eddy viscosity ratio and turbulence modification

Fig. 11 shows the relation between C_{TI}/N_d and Gore and Crowe's critical parameter. The data are widely scattered and very low turbulence augmentations are observed even in the region of $d/l_t > 1$. On the contrary, the eddy viscosity ratio ϕ gives a much better correlation as shown in Fig. 12. There is little difference in the correlation between gas–liquid and liquid–solid flows, and therefore the influence of non-spherical bubble shapes on the turbulence modification is negligible in the present experimental range. The critical point at which

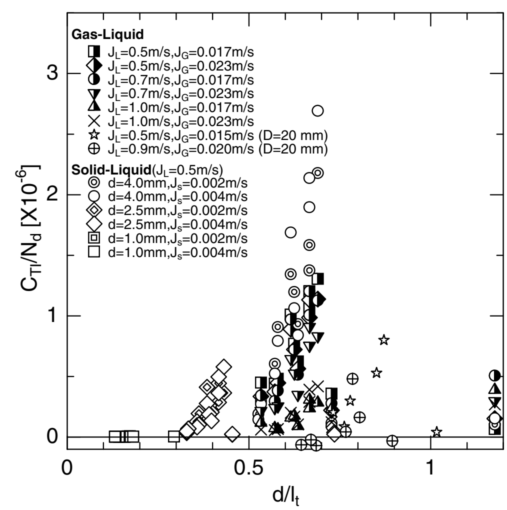

Fig. 11. Correlation between d/l_t and C_{TI}/N_d.

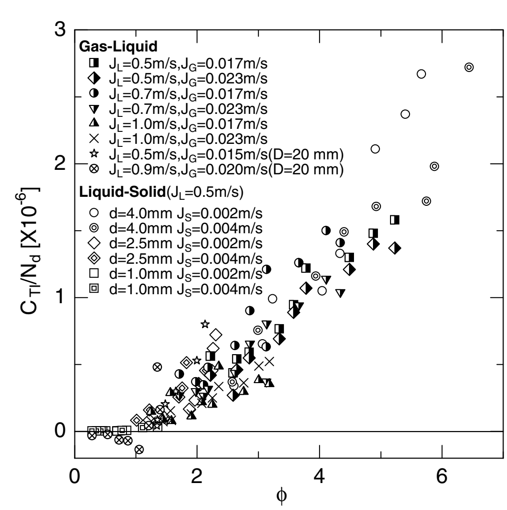

Fig. 12. Correlation between ϕ and C_{TI}/N_d.

no modification occurs is close to $\phi = 1$, irrespective of the type of two-phase dispersed flow. The eddy viscosity ratio is, therefore, the more appropriate parameter than d/l_t for correlating turbulence modification not only for gas–solid flows but also for gas–liquid and liquid–solid flows. It should be noted that the C_{TI}/N_d and ϕ plotted in Fig. 12 are local quantities at different radial positions. The magnitude of eddy viscosity ratio ϕ is equal to the product of Gore and Crowe's parameter d/l_t and u_r/u'. To examine the influence of u_r/u' to the turbulence modification, C_{TI}/N_d is plotted against u_r/u' as shown in Fig. 13. Though there is a positive correlation between u_r/u' and C_{TI}/N_d, the scatter of data in Fig. 13 is larger than that in Fig. 12. Figs. 11–13 clearly show that ϕ is a better parameter for correlating the turbulence modification than d/l_t and u_r/u'.

The correlations between C_{TI}/N_d and ϕ of gas–liquid and liquid–solid two-phase flows are compared with that of gas–solid two-phase flows (Hosokawa et al., 1998) in Fig. 14. The gradient of the correlation for gas–solid flows is much smaller than that for liquid–solid and gas–liquid flows, which indicates that the magnitude of turbulence modification depends on the fluid properties of the continuous phase. The most important fluid property relating with turbulence dissipation might be the kinematic viscosity. High kinematic viscosity would result in a high dissipation rate, and therefore, larger kinetic energy might be required to increase the turbulence intensity. Hence C_{TI}/N_d is multiplied by the ratio of the kinematic viscosity of the continuous phase to that of water (ν/ν_{water}). Here water is selected as a reference fluid. The result is shown in Fig. 15, which gives a much better correlation than the $C_{TI}/N_d - \phi$ plane. However, further experiments with various continuous fluids are definitely indispensable to confirm the applicability of $\nu/\nu_{water} C_{TI}/N_d - \phi$ plane to correlate the turbulence modification.

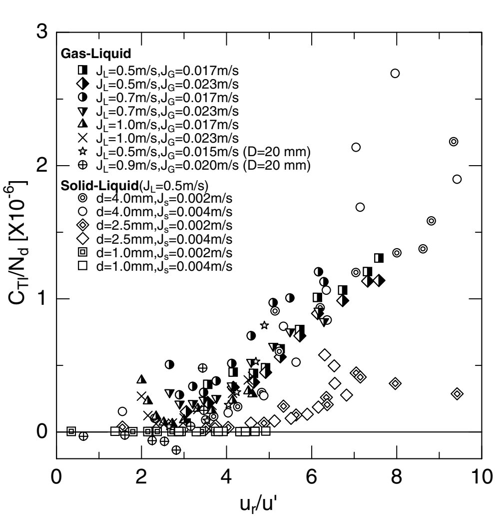

Fig. 13. Correlation between u_r/u' and C_{TI}/N_d.

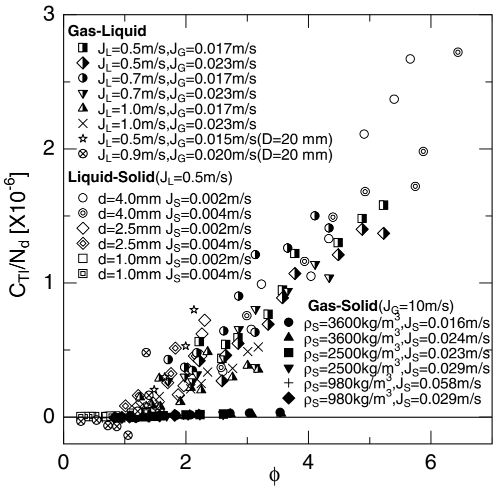

Fig. 14. Correlation between ϕ and C_{TI}/N_d in gas–liquid, liquid–solid and gas–solid two-phase flows.

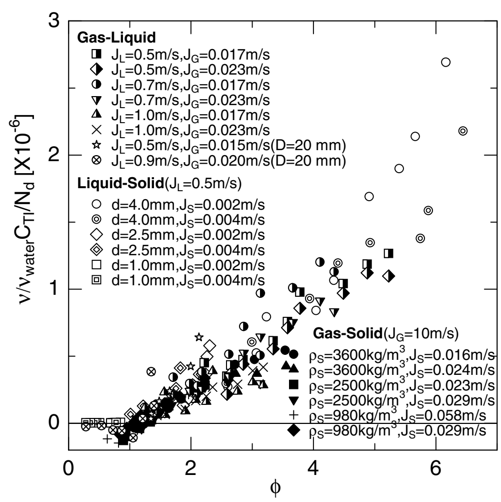

Fig. 15. Correlation between ϕ and $\nu/\nu_{water} C_{TI}/N_d$ in gas–liquid, liquid–solid and gas–solid two-phase flows.

For comparison with available experimental data (Lee and Durst, 1982; Tsuji et al., 1984), C_{TI} was integrated over the cross-sectional area of the pipe, and the mean change in turbulence intensity $\widetilde{C_{TI}}$ was defined by

$$\widetilde{C_{TI}} = \frac{\int_0^R 2\pi r \frac{u'}{\bar{u}}\,\mathrm{d}r - \int_0^R 2\pi r \frac{u'_t}{\bar{u}_t}\,\mathrm{d}r}{\int_0^R 2\pi r \frac{u'_t}{\bar{u}_t}\,\mathrm{d}r} \tag{16}$$

where r is the radial position and R the pipe radius. Since the diameters of dispersed phase in each experiment were more or less constant over the cross-sectional area, the area-averaged number density of the dispersed phase $\langle N_d \rangle$ was evaluated by using the area-averaged phase fraction of the dispersed phase $\langle \alpha_d \rangle$ and the mean diameter d of the dispersed phase as follows:

$$\langle N_d \rangle = \frac{6\langle \alpha_d \rangle}{\pi d^3} \tag{17}$$

The area-averaged RMS value in a single-phase flow $\langle u_t' \rangle$ was used to evaluate the area-averaged eddy viscosity ratio. Since the available experimental data provide only the mean velocities of continuous phase $\bar{u}(r)$ and dispersed phase $\overline{u_d}(r)$, the mean value of relative velocity $\widetilde{u_r}$ was evaluated by

$$\widetilde{u_r} = \frac{1}{\pi R^2}\left| \int_0^R 2\pi r(\bar{u}(r) - \overline{u_d}(r))\,\mathrm{d}r \right| \tag{18}$$

The integrated turbulence length scale in a single-phase flow is however an unknown parameter. Hutchinson et al. (1971) suggested that the ratio of l_t to R is constant over the cross section under the condition of $5.0 \times 10^4 < Re < 5.0 \times 10^5$. Since the measured l_t/D shown in Fig. 6 is about 0.2, the integrated turbulence length scale $\bar{l}_t$ of the single-phase flow was evaluated as $0.2D$. Thus, the mean eddy viscosity ratio $\tilde{\phi}$ was evaluated by

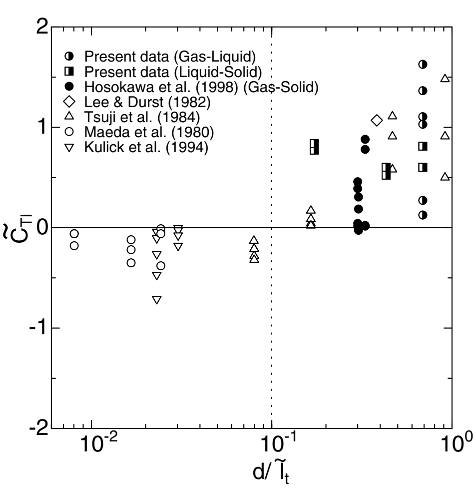

Fig. 16. Correlation between $d/\tilde{l}_t$ and $\widetilde{C_{TI}}$ (Gore and Crowe, 1989; some data are cited from Lee and Durst, 1982; Tsuji et al., 1984; Maeda et al., 1980; Kulick et al., 1994).

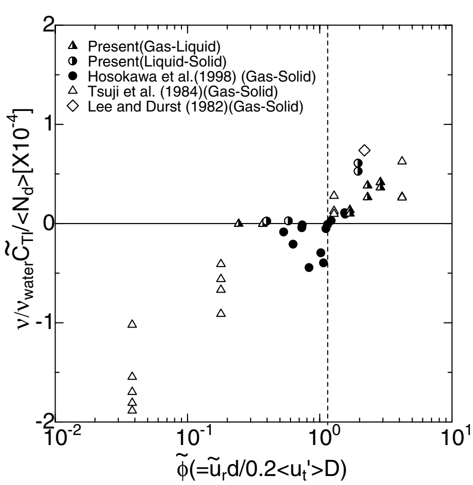

Fig. 17. Correlation between $\tilde{\phi}$ and $\nu/\nu_{\mathrm{water}}\widetilde{C_{TI}}/\langle N_d \rangle$.

$$\tilde{\phi} = \frac{\widetilde{u_r}\bar{d}}{0.2\langle u_t' \rangle D} \tag{19}$$

Fig. 16 shows the correlation between Gore and Crowe's parameter $d/\tilde{l}_t$ and $\widetilde{C_{TI}}$. The present data and available data are widely scattered. The relation between $\nu/\nu_{\mathrm{water}}\widetilde{C_{TI}}/\langle N_d \rangle$ and $\tilde{\phi}$ is plotted in Fig. 17. The scatter of the data in this plot is smaller, and a linear correlation is realized, in contrast to Fig. 16.

5. Conclusions

To examine whether or not the eddy viscosity ratio ϕ is applicable to gas–liquid and solid–liquid dispersed two-phase upflows in vertical pipes, velocities of continuous phase and dispersed phases were measured with LDV and an image processing method. Volumetric fluxes of liquid and dispersed phases, particle diameter and pipe diameter were chosen as the experimental parameters to examine the effects of the intensities of shear-induced and particle/bubble induced turbulence, the number density of the dispersed phase and the pipe diameter on turbulence modification. It was confirmed that the change in turbulence intensity per unit number density of dispersed phase C_{TI}/N_d is better correlated with ϕ than with Gore and Crowe's parameter. The critical point at which no modification occurs is close to $\phi = 1$, irrespective of the type of two-phase dispersed flow. The mean eddy viscosity ratio defined by Eq. (19) also well correlates with mean changes in turbulence intensity measured for various two-phase flows. The eddy viscosity ratio is, therefore, an appropriate parameter for correlating turbulence modification not only for gas–solid two-phase flows but also for gas–liquid and liquid–solid two-phase flows.

References

DANTEC, 1993. User's Manual Particle Dynamics Analyzer.

Delhaye, J.M., Giot, M., Riethmuller, M.L., 1981. Thermohydraulics of Two-phase Systems for Industrial Design and Nuclear Engineering. A von Karman Institute Book. Hemisphere.

Gore, R.A., Crowe, C.T., 1989. Effect of particle size on modulating turbulent intensity. Int. J. Multiphase Flow 15 (2), 279–285.

Gore, R.A., Crowe, C.T., 1991. Modulation of turbulence by a dispersed phase. Trans. ASME 113, 304–307.

Hosokawa, S.,Tomiyama, A., Morimura, M., Fujiwara, S., Sakaguchi, T., 1998. Influence of relative velocity on turbulence intensity in gas–solid two-phase flow in a vertical pipe. ICMF'98-Lyon CD-ROM.

Hinze, J.O., 1959. Turbulence. McGraw-Hill, New York.

Hutchinson, P., Hewitt, G.F., Dukler, A.E., 1971. Deposition of liquid or solid dispersion from turbulent gas streams: a stochastic model. Chem. Eng. Sci. 26, 419–439.

Kulick, J.D., Fessler, J.R., Eaton, J.K., 1994. Particle response and turbulence modification in fully developed channel flow. J. Fluid Mech. 277, 109–134.

Lance, M., Bataille, J., 1991. Turbulence in the liquid phase of a uniform bubbly flow. J. Fluid Mech. 22, 95–118.

Laufer, J., 1954. The Structure of Turbulence in Fully Developed Pipe Flow. NACA Report No. 1174.

Lee, S.L., Durst, F., 1982. On the motion of particles in turbulent duct flow. Int. J. Multiphase Flow 8 (2), 125–146.

Maeda, M., Hishida, K., Furutani, T., 1980. Velocity distributions of air–solid suspension in upward pipe flow (effect of particles on air velocity distribution). Trans. Jpn. Soc. Mech. Eng., Ser. B 46, 2313–2320.

Sato, Y., Sekoguchi, K., 1975. Liquid velocity distribution in two-phase bubbly flow. Int. J. Multiphase Flow 2, 79–95.

Serizawa, A., Kataoka, I., 1988. Phase distribution in two-phase flow. In: Afgan, N.H. (Ed.), Transient Phenomena in Multiphase Flow. Hemisphere, pp. 179–224.

Serizawa, A., Kataoka, I., 1995. Dispersed flow-I. Multiphase Sci. Technol. 7, 125–194.

Serizawa, A., Kataoka, I., Michiyoshi, I., 1975. Turbulence structure of air–water bubbly flow-II. Local properties. Int. J. Multiphase Flow 2, 235–246.

Townsend, A.A., 1956. The Structure of Turbulent Shear Flow. Cambridge University Press, New York.

Tsuji, Y., Morikawa, Y., Shiomi, H., 1984. LDV measurements of an air–solid two-phase flow in a vertical pipe. J. Fluid Mech. 139, 417–434.